

Can Membership Inferencing be Refuted?

Zhifeng Kong[§], Amrita Roy Chowdhury[§], Kamalika Chaudhuri
University of California, San Diego

Abstract—Membership inference (MI) attack is currently the most popular test for measuring privacy leakage in machine learning models. Given a machine learning model, a data point and some auxiliary information, the goal of an MI attack is to determine whether the data point was used to train the model. In this work, we study the reliability of membership inference attacks in practice. Specifically, we show that a model owner can plausibly refute the result of a membership inference test on a data point x by constructing a *proof of repudiation* that proves that the model was trained *without* x . We design efficient algorithms to construct proofs of repudiation for all data points of the training dataset. Our empirical evaluation demonstrates the practical feasibility of our algorithm by constructing proofs of repudiation for popular machine learning models on MNIST and CIFAR-10. Consequently, our results call for a re-evaluation of the implications of membership inference attacks in practice.

Modern, complex machine learning models are known to leak sensitive training data [43]. Membership inference (MI) attack [51] has emerged as the primary metric for measuring privacy leakage for machine learning models. For instance, government organizations such as the ICO (UK) and NIST (US) currently highlight membership inference as a potential confidentiality violation and privacy threat to the training data [38]. Given a model M_θ trained on a dataset D , a target data point x^* , and some auxiliary information, the goal of an MI attack is to predict whether the data point x^* was used to train the model M_θ . A large body of prior work [11], [12], [28], [63], [54], [59] has developed effective MI attacks and used them to characterize the privacy leakage for different models. Additionally, MI attacks have been deployed in practice for privacy audits – for example, in the privacy testing library of TensorFlow [3].

Given its widespread popularity, analyzing the reliability or well-posedness of a membership inference attack is of immense practical importance. Suppose an adversary carries out a successful membership inference attack on a data point x^* – is this sufficient to indisputably argue that x^* was indeed used to train the model M_θ ? We take a closer look at this problem in this paper and ask the specific question:

Can a model owner refute a membership inferencing claim in practice?

The main challenge here is how can a model owner plausibly assert such a repudiation. We propose to do this as follows. Given a model M_θ trained by stochastic gradient descent (SGD) on a training dataset D and a target data point $x^* \in D$, we present a proof that it is computationally feasible for the

model owner to have generated the *same model from a different dataset* $D' = D \setminus \{x^*\}$ that does not contain the data point x^* . We call this a *Proof-of-Repudiation (PoR)*. The proof of repudiation empowers a model owner to plausibly deny the membership inferencing prediction and present a counter claim that x^* is in fact *not* a member. This discredits the predictions of an MI attack. Thus, an adversary cannot “go-to-court” with the prediction of an MI attack.

For the concrete construction, we use a log that records the entire training trajectory (i.e., the sequence of SGD updates including all the relevant training details, such as mini-batch indices and model weights) starting from the initialization to the final model weights. Any third-party entity can reproduce the steps of gradient descent from the log and verify the validity of the sequence provided. Specifically, the model owner produces a “forged” log showing the model’s training trajectory on a dataset $D' = D \setminus \{x^*\}$ and uses it as a proof of repudiation for refuting membership inference claims on x^* . This suffices to raise a *reasonable doubt* on the adversary’s claim. The above construction is based on the notion of *forgeability* which was introduced by Thudi et al. [57] in the context of machine unlearning (Section I-D). An attractive aspect of our construction is that the generated PoR is completely *agnostic* of the MI attack. Additionally, it requires *no* modifications to the model’s training and inference pipeline.

In this paper, we aim to produce proofs of repudiation for all the data points of the training dataset. A naive approach is to repeat the construction by Thudi et al. [57] on every data point. However, there are two challenges with this approach. First, this is extremely computationally inefficient especially for modern models trained on huge datasets. Second, their approach cannot accommodate modern sophisticated training techniques, such as data augmentation.

We address both challenges through a series of algorithmic innovations. First, we provide a way to strategically reuse certain information – “forged” mini-batches as well as proofs of repudiation – across multiple training data points, which improves efficiency by three orders of magnitude. Second, we extend support for a popular data augmentation technique known as the Random Flip augmentation by using additional transformation information. Combining these techniques gives us a practical proof-of-repudiation generation algorithm that can be run on popular models on standard datasets, such as MNIST and CIFAR-10, even with academic computational resources.

[§]The first two authors have made equal contributions.

We empirically evaluate our algorithm on three popular models trained on two standard datasets – MNIST and CIFAR-10. Our results indicate that it is possible to generate valid proofs of repudiation for at least 98.8% and 87.8% of the data points of MNIST and CIFAR-10, respectively. We measure the quality of the proofs by evaluating them against five standard ML attacks, including state-of-the-art attacks such as LiRA [12] and EnhancedMIA [62], which are specifically designed to maximize prediction accuracy under a *low* false positive regime. We see that our algorithm can fool even these attacks, and performs remarkably well in practice. Additionally, we analyze the limitations of proofs of repudiation and observe that one cannot generate a valid proof for outlier/out-of-distribution data points. We provide a formal impossibility result for linear models (Theorem 1).

Since proofs of repudiation enable a model owner to refute a membership inference claim *post-attack*, our results question the reliability of ML attacks in practice, and call for a re-evaluation of how they are used in measuring the privacy leakage of ML models. We argue that ML attacks are perhaps better suited for distinguishing between in- and out-of-distribution data points in practice (see Sections III-B and VI). Making reliable inferencing on in-distribution data points would require a new lens of investigation.

I. BACKGROUND

A. Machine Learning

Machine learning (ML) is the task of learning model M_θ from a dataset where θ denotes the parameters of the model. Here, we focus on supervised learning where the dataset D consists of points $(x_i, y_i) \in \mathcal{X} \times \{1, \dots, c\}$, where $y_i \in \{1, \dots, c\}$ is the label of the input $x_i \in D$, and there are c possible labels. The goal of supervised ML is to predict the label y of an unlabelled input x by using the knowledge learned from the labeled dataset D . Let L be the loss function. Let g be the update rule that takes the model θ_t and a mini-batch $(\hat{x}^{(t)}, \hat{y}^{(t)})$ of size b at step t as inputs, and updates the model parameter as $\theta_{t+1} = g(\theta_t, (\hat{x}^{(t)}, \hat{y}^{(t)}))$. In this paper, we focus on the SGD update rule. At each t , $(\hat{x}^{(t)}, \hat{y}^{(t)})$ is uniformly selected from D without replacement, and the update rule is

$$\theta_{t+1} = \theta_t - \text{step_size} \cdot \frac{1}{b} \sum_{i=1}^b \frac{\partial L(M_\theta(\hat{x}_i^{(t)}), \hat{y}_i^{(t)})}{\partial \theta} \Bigg|_{\theta=\theta_t} . \quad (1)$$

For conciseness, in the rest of the paper, we drop the notation y for labels and represent a sample by x , and let $\hat{x} \in D$ denote a mini-batch of size b sampled from D .

B. Membership Inference Attacks

The goal of a membership inference (MI) attack [51], [11], [12], [28], [63], [54], [59] is to predict whether a data point was used in training a given model. MI attacks are currently the most widely deployed attack for auditing privacy of machine learning models. We consider a model owner who has trained

a ML model M_θ on a dataset D . Both the model M_θ and the dataset D is proprietary to the model owner.

Prior work [12], [28], [63] has made attempts at formalizing the MI attack along the lines of a security game which is inspired by cryptography. The attack takes the model M_θ , a data point drawn from the input distribution $x^* \sim \mathbb{D}$, possibly some auxiliary knowledge ψ (for instance, query access to the distribution \mathbb{D}) and outputs its prediction bit $b \leftarrow \mathcal{A}(x^*, M_\theta, \psi)$ indicating its belief about x^* 's membership. The security games are played between two parties – the challenger \mathcal{C} and the adversary \mathcal{A} . For the MI attack, the model owner acts as the challenger and the security game, $\mathcal{G}_{MI}(\cdot)$, is defined as follows:

Definition 1 (Membership Inference Security Game ($\mathcal{G}_{MI}(\cdot)$)). The membership inference attack is defined as follows:

- 1) The challenger \mathcal{C} samples a dataset $D \sim \mathbb{D}$ via a *fixed* random seed, S_D , and trains a model $M_\theta \leftarrow \mathcal{T}(D)$ on it by using a fixed random seed, $S_{\mathcal{T}}$, in the training algorithm $\mathcal{T}(\cdot)$.
- 2) The challenger \mathcal{C} flips a bit b , and if $b = 0$, samples a fresh challenge point from the distribution $x^* \sim \mathbb{D}$ (such that $x^* \notin D$). Otherwise, the challenger selects a data point from the training set $x^* \leftarrow D$. The challenger uses a fresh random seed S_{x^*} for both the cases.
- 3) The challenger \mathcal{C} sends x^* to the adversary \mathcal{A} .
- 4) Let ψ denote the adversary's auxiliary knowledge (for instance, query access to the distribution \mathbb{D}). The adversary outputs a bit $b' \leftarrow \mathcal{A}(x^*, M_\theta, \psi)$.
- 5) Output 1 if $b' = b$, and 0 otherwise.

In the above game, fixing the random seeds, S_D and $S_{\mathcal{T}}$ imply that the challenger always trains the *same* model M_θ from the *same* dataset D . We choose this particular setting because this captures the real-world scenario of a typical ML model post-deployment (setting 2 as discussed later). There can be a couple of variations of the above game based on the (fixed or fresh) instantiation of the random seeds, S_D , $S_{\mathcal{T}}$, and S_{x^*} (see [62] for more details).

Typically, MI attacks have been studied under the following two settings:

Setting 1. MI attacks are used for *auditing* privacy internally *pre-deployment*. Here, the model owner acts as both the challenger and the adversary in the game and carries out MI attacks to stress-test the model privacy for data protection impact assessment [1]. The success rate of the MI attacks is used to assess the privacy leakage from M_θ about its training dataset D .

Setting 2. The second setting deals with practical threat that an MI attack poses for a ML model *post deployment*. In the above game, the adversary here is a real-world attacker who

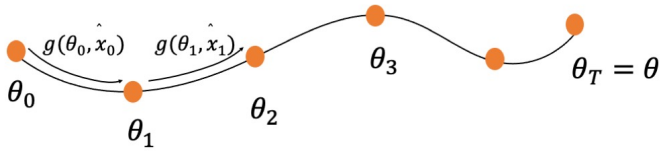


Fig. 1: PoL records the training trajectory, i.e., sequence of SGD updates, of a model M_θ .

tries to infer sensitive membership information and act on it (see Section VI for some illustrative examples).

Our results have *no* bearing on the first setting of using MI attacks for internal privacy audits pre-deployment. For the rest of the paper, we are only interested in the second setting – refuting membership inference claims of a real-world MI attack.

Note that we consider a white-box MI attack construction where we assume that the adversary \mathcal{A} has access to the full model M_θ to capture the most general setting. However, restricting the adversary to only a black-box access to the model (for instance, in the case of ML-as-a-Service platforms) does not affect any of the discussion in this paper.

C. Proof-Of-Learning (PoL)

The concept of Proof-of-Learning (PoL) was introduced by Jia et al. [29]. It enables an entity to provide evidence that they have

- performed the necessary computation on a dataset D to train a model M_θ , and that
- all the steps have been performed correctly.

Consequently, PoL allows the verification of the integrity of the training procedure used to obtain M_θ by a third-party authority, such as a regulator. It was proposed in the context of establishing model ownership, or verifiable outsourcing of model training. The core idea is to maintain a log throughout training which facilitates reproduction of the alleged computations the entity carried out. A valid PoL log is formally defined as follows:

Definition 2 (Proof-of-Learning (PoL) [29]). Recall, $g(\theta, \hat{x}) = \theta'$ denotes updating the model parameters θ to θ' where g is a training algorithm/update rule. A valid Proof-of-Learning (PoL) log, (g, d, ϵ) is a sequence of $\{(\theta_i, \hat{x}_i)\}_{i \in J}$ for some countable indexing set J , such that $\forall i \in J, d(\theta_{i+1}, g(\theta_i, \hat{x}_i)) \leq \epsilon$ for some training function g and metric d on the parameter space. The threshold ϵ is a tolerance parameter for the verification.

From the above definition, the PoL documents intermediate checkpoints of the model, data points used, and any other information required for the updates during training (for instance, hyperparameters that define the update rule at each step). The verifier checks a PoL’s validity by reproducing the

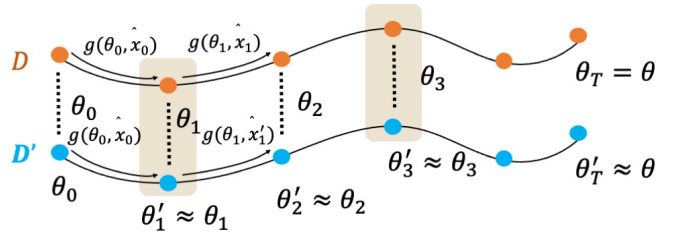


Fig. 2: Forgeability allows replacing data points from D by points from D' while keeping the model updates computed on these points (almost) identical .

t -th intermediate checkpoint of the model based on the information given in the log, including the $(t - 1)$ -th checkpoint, data points used at this step, and the same update rule as defined in the log. Then the verifier computes the distance between the t -th checkpoint in the log and the reproduced t -th checkpoint in the parameter space. This distance is called the verification error, and we say this update is valid if the verification error is below a certain threshold. For the rest of the paper, we use the ℓ_2 -distance as our distance metric d .

D. Forgeability

Privacy regulations such as GDPR [1] and CCPA [2] empower individuals with the Right to Deletion or Right to be Forgotten wherein a data owner who had previously allowed the use of their personal data can later retract the authorization. In the context of ML models, this requires the model owner to perform *machine unlearning* [8] to scrub the effect of the data point from the model. Machine unlearning is the mechanism of proving to the data owner that the model, which had originally been trained on their data, has been modified to “forget” whatever it might have learned from the data.

Forgeability [57] was introduced in the context of machine unlearning. In what follows, we present a simplified description of the original proposal which is relevant for understanding our paper.

Two datasets are defined to be forgeable w.r.t a given model if the same model parameters (up to some small per-step error) can *feasibly* be obtained by using either of the datasets. Here, feasibility is defined in terms of the PoL logs.

Definition 3 (Forgeability [57]). For two datasets D and D' , and PoLs stemming from the same model M_θ , we say D' forges D (with error ϵ'), if we have

$$\forall i, \exists \hat{x}'_i \in D', s.t. \quad (2)$$

$$d(\theta_{i+1}, g(\theta_i, \hat{x}'_i)) \leq \epsilon'. \quad (3)$$

Intuitively, forgeability means that the data points (mini-batches) of D can be mapped to data points of D' such that the parameter space is preserved (upto ϵ) as determined by a PoL log. Thus, we can replace the data points in D with that in D' and still obtain a valid PoL for the same model

M_θ (up to an error of ϵ'). Thus, forgeability is the ability to replace data points from one dataset by data points from another dataset while keeping the model updates computed on these data points (almost) identical.

Consequences for Machine Unlearning. In the context of machine unlearning, the authors present an algorithm (Algorithm 1) to generate PoL logs for carrying out the forging attack. The algorithm forges a dataset D with its subset dataset $D \setminus \{x_-\}$ where $x_- \in D$ is the data point to be deleted. For this, the algorithm randomly samples μ number of candidate mini-batches that do not contain x_- (Step 4-5). Then, it chooses the one that minimizes the ℓ_2 -distance between gradients computed from candidate and original mini-batches (Step 6-8). We call this the forged mini-batch, $B_{\text{forge}}^{(t)}$ and this step is repeated for every training iteration $t \in [\tau]$. All the τ forged mini-batches constitute the forged PoL.

II. PROOF-OF-REPUDIATION (PoR)

In this section, we formalize our problem statement.

Problem Statement. Consider a scenario where a real-world adversary carries out an MI attack on a model M_θ trained on dataset D and correctly predicts that a point $x^* \in D$ is indeed a member of the training dataset. This corresponds to the second setting as discussed in Section I-B. Given the above scenario, the question we study here is that can the model owner now repudiate the adversary’s membership inference claim on x^* . We show that the ability to forge (Section I-D) enables the model owner to construct a *Proof-of-Repudiation* (PoR) which empowers them to *repudiate* the prediction. The PoR enables the model owner to plausibly deny the MI prediction and present a counter claim that x^* is in fact *not* a member. This discredits the predictions of an MI attack.

A. Definition of a PoR

Next, we provide the formal definition of PoR.

Definition 4 (Proof Of Repudiation (PoR)). Let M_θ be a ML model trained on a dataset D . A valid proof-of-repudiation $\mathcal{P}(M_\theta, D, x^*)$ for a membership inferencing claim on a data point $x^* \in D$ is a certificate to the effect that it is computationally *feasible* for the model owner to have obtained the *same* model M_θ from a *different* dataset D' such that $x^* \notin D'$.

From the above definition, given a model M_θ and a membership inference claim that data point x^* is a member of its training dataset D , a valid PoR should provide evidence that the model owner could have obtained the model M_θ from a different dataset D' that does *not* contain the data point x^* . Clearly, a certificate to the above effect suffices to raise a *reasonable doubt* on the membership inference claim on x^* . In other words, the adversary now *cannot* claim with absolute certainty that x^* was indeed a member of the training dataset D . Next, we describe a set of desirable properties of a PoR.

- **P1. Correctness.** The PoR should be verifiable with very high probability, i.e., the reported computation (concern-

ing the training of M_θ) should be reproducible by any third-party verifier.

- **P2. Attack Agnostic.** PoR should be completely agnostic of the MI attack used for making the prediction, i.e., the *same* PoR should be valid for *all* MI attacks as long as they all have the make the same prediction ($b = 1$) on x^* .
- **P3. Model Agnostic.** PoR should be agnostic of specificities of the ML model, such as model architecture, number of parameters.
- **P4. Proof Generation Efficiency.** A challenger \mathcal{C} should be able to generate the PoR efficiently. Specifically, not too much extra effort than training the algorithm.
- **P5. Proof Verification Efficiency.** The PoR verification should be efficient and ideally less computationally expensive than generating the PoR. Additionally, verification should succeed even on a different hardware than the one used for generation.

III. HOW TO CONSTRUCT A PoR?

In this section, we describe the construction of a PoR. For this, first we introduce a practical relaxation of a PoR followed by its construction leveraging forgeability.

For the rest of the paper, we consider the dataset $D' = D \setminus \{x^*\}$, i.e., the original dataset with only the data point in contention, x^* , removed. As indicated in Definition 4, we can conclude that an MI attack is infeasible for an input data point $x^* \in D$ if we can *prove* that both the datasets D and D' can generate the exact *same* model, M_θ . However here, we relax this assumption and allow the two models – the one obtained from training on D , M_θ , and the other from D' , M'_θ to differ by a small amount ϵ^* . Specifically, we mean that the parameters of the two models, M_θ and M'_θ can differ from each other by at most ϵ^* – we denote this by $\|\theta - \theta'\|_2 \leq \epsilon^*$. Based on this relaxation we define the notion of *membership inference equivalence* with respect to an MI attack as follows. Recall, that the output of an attack is a bit, $\mathcal{A}(x, M_\theta, \psi) = b$, indicating the adversary’s belief on whether the point belongs to the dataset.

Definition 5 (Membership Inference Equivalence). For a given distribution \mathbb{D} , two models $\{M_\theta, M'_\theta\}$ are defined to be functionally equivalent w.r.t to an MI attack (adversary), \mathcal{A} iff,

$$\forall x \in \mathbb{D}, \mathcal{A}(x, M_\theta, \psi) = \mathcal{A}(x, M'_\theta, \psi). \quad (4)$$

From the above definition, two models are membership inference equivalent w.r.t an MI attack if the MI attack’s prediction remains the *same* on both the models for all the points in the data distribution \mathbb{D} . In other words, the two models are equivalent in terms of the functionality of the attack. We argue that this relaxation is justified because in

Algorithm 1 Generation of forged PoL ([57])

- 1: **Inputs:** $D = \{x_1, \dots, x_n\}$ - Training dataset; τ - Total number of iterations; $B_*^{(t)}$ - Training mini-batches for the t -th iteration where $t \in [\tau]$; b - Size of each mini-batch, $|B_*^{(t)}|$; $\theta^{(0)}$ - Initialization parameters; x_- - Data point to be deleted.
- 2: **Hyper-parameters:** `step_size`; μ - Number of candidate mini-batches sampled per iteration for forging.
- 3: **for** $t = 1, \dots, \tau$ **do**
- 4: Randomly select a subset D_{sub} from $D \setminus \{x_-\}$.
- 5: Randomly select μ mini-batches of size b from D_{sub} : $B_1^{(t)}, \dots, B_\mu^{(t)}$.
- 6: Compute gradients and update the original model:

$$\text{grad}^{(t)} = \frac{1}{b} \nabla_{\theta} \sum_{x \in B_*^{(t)}} \ell(x; \theta^{(t)}); \quad \theta^{(t)} = \theta^{(t-1)} - \text{step_size} \cdot \text{grad}^{(t)}.$$

- 8: Choose the best mini-batch to approximate the gradient:
- 9:

$$m_*^{(t)} = \arg \min_{m \in [\mu]} \left\| \frac{1}{b} \nabla_{\theta} \sum_{x \in B_m^{(t)}} \ell(x; \theta^{(t)}) - \text{grad}^{(t)} \right\|_2^2.$$

- 10: $B_{\text{forge}}^{(t)} = B_{m_*^{(t)}}^{(t)}$.

- 11: **end for**

- 12: **Return:** original model $\theta_* = \theta^{(\tau)}$; all forged mini-batches $\{B_{\text{forge}}^{(t)} : t \in [\tau]\}$.
-

practice, a membership inferencing is defined by the attack functionality. One can consider this relaxation to be analogous to the assumption of computationally bounded adversaries in cryptography since in practice, adversaries are always computationally bounded. Similar assumptions have also been made in differential privacy – Chaudhuri et al. [15] proposed capacity-bounded differential privacy where the adversary that distinguishes the output distributions is assumed to be bounded in terms of the function class from which their attack algorithm is drawn. We refer to M'_θ as the forged model in the rest of the paper. Based on this, we propose the following conjecture.

Conjecture 1. For some small value of ϵ' , if $\|\theta - \theta'\|_2 \leq \epsilon'$, then the two models $\{M_\theta, M'_\theta\}$ are membership equivalent w.r.t an MI attack.

The above conjecture states that if two models are sufficiently close to each other in the parameter space, then they are functionally equivalent w.r.t MI attacks. The intuitive reasoning behind this is that models that are very close to each other in the parameter space result in very similar scores for an MI attack leading to the same prediction.

Based on the above relaxation, the PoR now should be able to prove that it is computationally feasible for the model owner to have generated *almost the same* model, M'_θ , from a different dataset D' . Now recall that a PoL (Section I-C) for any model M_θ trained on any dataset D logs its complete training trajectory, (i.e., sequence of SGD model updates). Reproducing the alleged computation is synonymous to showing its plausibility. This clearly establishes the *computational feasibility* of obtaining M_θ from the dataset D . Hence, for the rest of paper we use PoLs to establish computational

feasibility.

Now note that the model owner (challenger) who has trained M_θ on the dataset D automatically has access to the PoL for the original dataset D . Based on our above discussion, the construction of a PoR for data point x^* reduces to generating a PoL for the model M'_θ for the dataset $D' = D \setminus \{x^*\}$. This is exactly what is enabled by forgeability (Section I). Specifically, forgeability allows the model owner to create a forged PoL for $\langle M'_\theta, D' \rangle$ from the original PoL for $\langle M_\theta, D \rangle$ such that $\|\theta - \theta'\|_2 \leq \epsilon'$ for some tolerance parameter ϵ' . Thus, the model owner can re-purpose a forged PoL for $\langle M'_\theta, D \setminus \{x^*\} \rangle$ as a PoR for refuting a membership inference claim on x^* . This completes our construction of a valid PoR.

A. Algorithm for PoR Generation

In this section, we describe the algorithm to construct PoRs in practice. Let $D = \{x_1, \dots, x_n\}$ be the set of training data. Let the original model be trained with τ iterations, where $B_*^{(t)}$ is the mini-batch used for the t -th iteration, $t \in [\tau]$. The goal is to generate n PoRs (i.e., forged PoLs) from $D'_{-i} = D \setminus \{x_i\}$ for all $i \in [n]$. Recall that a forged PoL from D'_{-i} is a sequence of mini-batches $\{B_{\text{forge}}^{(t)}(x_i)\}$ such that

- $x_i \notin B_{\text{forge}}^{(t)}(x_i)$, and
- For each iteration t , the gradient of the model using $B_{\text{forge}}^{(t)}(x_i)$ closely approximates the gradient computed from the original mini-batch $B_*^{(t)}$.

The naive strategy is to run Algorithm 1 [57] iteratively and generate n forged PoLs. However, it has the following limitations:

- **Computation cost.** It needs to compute $n \cdot \mu \cdot \tau$ gradients in total (Step 3-9 in Algorithm 1), where μ is the number of candidate mini-batches (see Section I-D). This is computationally expensive when n is large.
- **Limited applicability.** The proposed algorithm works only for the simple update rules and cannot accommodate more complex training techniques such as data augmentation.

To address these challenges, we propose an improved two-phase mechanism to generate the PoRs. In the first phase, we compute and store the forged mini-batches $B_{\text{forge}}^{(t)}(x_i)$ for all data points $i \in [n]$ and iterations $t \in [\tau]$ using . We propose an efficient algorithm (Algorithm 2) to do this, and it is able to handle more complex training techniques.

The second phase is to reconstruct the PoR from stored information *on-the-fly*. This step is done when the model owner is challenged with a membership inference claim from an attacker post-deployment. With the two-step mechanism we can avoid saving the entire PoRs (including all details, such as model parameters for every iteration) during the training phase, which requires prohibitively large storage costs and I/O burden especially for modern, big ML models.

Our mechanism is based on three key ideas as follows:

Key Idea 1: Re-using Forged Mini-batches. To reduce the overhead of expensive gradient computation, we propose to *re-use forged mini-batches* across PoRs. For each iteration $t \in [\tau]$, we randomly split the training dataset into κ subsets, $D_1^{(t)}, \dots, D_\kappa^{(t)}$, where κ is a hyper-parameter with a small value (for instance, $\kappa = 5$) independent of n . These subsets are equi-sized and disjoint:

$$|D_k^{(t)}| = n/\kappa; D_k^{(t)} \cap D_{k'}^{(t)} = \emptyset \text{ when } 1 \leq k \neq k' \leq \kappa. \quad (5)$$

For the t -th iteration, we randomly sample μ candidate mini-batches from $D \setminus D_k^{(t)}$ and store the one that best approximates the original gradient. For all $x_i \in D_k^{(t)}$, we let choose this as the forged mini-batch $B_{\text{forge}}^{(t)}(x_i)$. In this way, the number of gradient computations is reduced to $\kappa \cdot \mu \cdot \tau$.

Key Idea 2: Combining PoRs. The second step in our mechanism is to reconstruct all n PoRs and thus requires $n \cdot \tau$ gradient computations. In order to further reduce the computation overhead, we partition the training data into groups of size λ . For each group $\hat{X}_i, i \in [n/\lambda]$, we compute the PoR from $D \setminus \hat{X}_i$. The computed PoR can thus work for *all* λ data points in \hat{X}_i . To achieve this, we require for any $i \in [n/\lambda]$ at any step $t \in [\tau]$, the λ samples

$$\hat{X}_i \subset D_k^{(t)}. \quad (6)$$

for some $k \in [\kappa]$. This reduces the number of PoRs to be generated to n/λ , and therefore reduces the number of gradient computes in the reconstruction phase to $n \cdot \tau/\lambda$.

Key Idea 3: Extension to Practical Techniques. Data augmentation is frequently used in practice during model training for improving the model accuracy and generalization. This constitutes augmenting with original training dataset with data points with random transformations. To extend our algorithm to models trained with data augmentation, we let training mini-batches $B_*^{(t)}$ to contain not only the indices but also information about the specific transformations applied. After selecting the μ candidate mini-batches in our algorithm, we apply the same data augmentation to these mini-batches and proceed. Specifically, we consider the common *random horizontal flip* augmentation, which randomly flips an image with 0.5 probability. We store a binary flag along with each sample index to indicate whether the corresponding sample is flipped.

In addition to data augmentation, certain modifications to the SGD update rule can also boost model performance in practice. Three common techniques are: momentum, weight decay, and learning rate scheduling. We extend our algorithm to support these techniques as follows. (1) Momentum in SGD means the update rule not only considers the current gradients but also those in the previous step. We do not modify the way to generate the PoR because we assume the gradients of forged mini-batches in the previous step are close to the true gradients in the previous step. We use the new update rule when reconstructing forged models. (2) Weight decay means there is an ℓ_2 regularization term of the model parameters in the loss function. We use the new loss function to compute gradients of the original and forged mini-batches. (3) Learning rate scheduling means the learning rate `step_size` changes during training. We use the corresponding learning rates when reconstructing the forged models.

Summary. The construction of our mechanism is outlined in Algorithm 2, where **orange lines** refer to modifications we make to the original Algorithm 1. The full algorithm that includes all practical techniques is presented in Algorithm 3 in Appendix B. The total number of gradient computation in our algorithm is $\kappa \cdot \mu \cdot \tau + n \cdot \tau/\lambda$. It is much more efficient than directly applying Algorithm 1 to all training samples, which requires $n \cdot \mu \cdot \tau$ gradient computes.¹

Discussion. Here we discuss how the proposed PoR construction meets the desiderata listed in Section II-A. At the core of a PoR is a log of the training trajectory which can be easily replicated and verified (upto a tolerance parameter) which satisfies **P1**. **P2** is met since the proposed construction of the PoR is completely attack agnostic. Given a target data point x^* , the same PoR works for *any* MI attack – even one with very a high confidence or low false positive rate (see Section IV). The PoR generation introduces no

¹For example, by taking $n = 5K, \mu = 200, \kappa = 5, \lambda = 10$, our algorithm is $1667 \times$ faster.

modifications² to the training pipeline thereby satisfying **P3**. A model owner who trains the model would have access to its training trajectory by default, enabling them to construct a PoR efficiently. Additionally, our proposed Algorithm 2 shows how we can piggyback the PoR generation process with the model training for efficient generation of PoRs for all the data points. This satisfies condition **P4**. For **P5**, instead of recomputing the gradient for *every* update step recorded in the log, the verifier can check the correctness of only a *subset* of the update steps. This allows the verifier to trade-off the confidence of verification with its computational cost – greater the number of updates steps checked, higher is the confidence in the proof’s validity. As suggested in [29], a heuristic could be to check the validity of only the largest model updates. The tolerance parameter can be set up to account for the errors incurred due to the usage of different hardware.

B. Can membership inferencing be always refuted?

It is important to note that PoRs have limitations in practice – we *cannot* create a valid PoR for *all* possible data points. We provide a formal impossibility result for a logistic regression model as follows.

Theorem 1. *Let $f(x) = \text{sigmoid}(w^\top x)$ with weight vector w . Let $\text{loss}(\cdot)$ be the cross entropy loss in Logistic regression. Assume x_2, \dots, x_n all lie on a subspace Γ and $x_1 \notin \Gamma$. Let the batchsize of SGD be 1 and $y_1 \neq \text{sigmoid}(w^\top x^*)$. Under the above condition, it is impossible to generate a valid PoR using Algorithm 2.*

Proof. The gradient at x_i is

$$\nabla_w \text{loss}(x_i) = (\text{sigmoid}(w^\top x_i) - y_i) x_i.$$

Then,

$$\begin{aligned} & \min_{2 \leq i \leq n} \|\nabla_w \text{loss}(x_1) - \nabla_w \text{loss}(x_i)\| \\ & \geq \min_{c \in \mathbb{R}, x \in \Gamma} \|cx - (\text{sigmoid}(w^\top x_1) - y_1) x_1\| \quad (7) \\ & \geq |\text{sigmoid}(w^\top x_1) - y_1| \text{dist}(x_1, \Gamma) > 0. \end{aligned}$$

Thus, clearly no sample from $D \setminus \{x_1\}$ can produce the same gradient as x^* , thus violating the assumption of Lemma 4 in [57] which is key for generating a PoL. \square

Another instance where one cannot refute a membership inferencing claim is the extreme case when the adversary knows all but one data point in D . We also cannot hope to create a valid PoR for an outlier/ out-of-distribution data point x^* . It is because, recall that the key idea of generating the PoR (i.e., forged PoL) is to replace a mini-batch B involving x^* with another B_{forge} such that $x^* \notin B_{\text{forge}}$ and the gradients of both are (almost) the same. However, for outliers it might not be possible to find appropriate alternative mini-batches

²A PoR can be generated on-the-fly as long as the model owner maintains a log of the gradient descent update trajectory during training. We propose Algorithm 2.2 for pre-computing the forged mini-batches only to reduce computational cost of generating the PoRs for all the data points in D .

in the dataset $D \setminus \{x^*\}$ such that the resulting gradients are sufficiently close.

IV. CAN WE CONSTRUCT VALID PORs IN PRACTICE?

In this section, we empirically evaluate whether valid PoRs can be constructed in practice. Recall that the core technique behind the construction of a PoR is forging a PoL.

To this end, we study the following three questions:

- **Q1.** What is the quality of the forged PoLs?
- **Q2.** What is the impact of the different algorithmic hyperparameters on the quality of forging?
- **Q3.** Do the forged mini-batches have the same distribution of samples as that of the original ones?

A. Experimental Setup

Datasets and Models. We look at two image datasets, *MNIST* [35] and *CIFAR-10* [33].

For *MNIST* [35], we train a *LeNet5* [34] model with 61.7K parameters. We use `step_size` = 1×10^{-2} , batch size $b = 100$ and 20 training epochs. The default values of the number of candidate mini-batches is $\mu = 200$ and number of random splits is $\kappa = 5$.

For *CIFAR-10* [33], we look at two models: *ResNet-mini* [22] with 1.49M parameters, and *VGG-mini* [53] with 5.75M parameters. We set `step_size` = 1×10^{-2} , batch size $b = 100$, and number of training epochs = 20. All models are augmented with random horizontal flips data augmentation, where each data point is randomly flipped with probability 0.5 each time. In addition to the standard SGD update rule, we study a modified SGD setting as introduced in Section III-A. We use notation \dagger to represent this setting. Specifically, we set momentum to be 0.9, weight decay coefficient to be 5×10^{-4} , and use cosine anneal for the learning rate scheduling (see Appendix C for details). We set the number of candidate mini-batches as $\mu = 200$ and number of random splits as $\kappa = 2$.

Experiment Design. Recall that the construction of a valid PoR constitutes

- **Condition 1.** Forging a PoL for $\langle M'_\theta, D' \rangle$ where $\|\theta - \theta'\|_2 < \epsilon'$ such that ϵ' is reasonably low.
- **Condition 2.** Ensuring that the models M_θ and M'_θ satisfy membership inference equivalence.

The goal of the experiments in this section is to generate a PoR for each point in D and check how many of them are actually valid, i.e., satisfy the aforementioned criterion. The naive mechanism is to generate n distinct PoRs, one for each data point. However, the resulting overhead would be very high and is beyond the computational powers of our academic resources. Hence, we explore two alternatives that approximates this ideal:

Algorithm 2 Generation of PoRs (simplified; see complete algorithm in Appendix B)

1: **Inputs:** $D = \{x_1, \dots, x_n\}$ - Training dataset; τ - Total number of iterations; $B_*^{(t)}$ - Training mini-batches for the t -th iteration where $t \in [\tau]$; b - Size of each mini-batch, $|B_*^{(t)}|$; $\theta^{(0)}$ - Initialization parameters.

2: **Hyper-parameters:** `step_size`; κ - Number of splits; μ - Number of candidate mini-batches sampled every iteration for forging.

3: **for** $t = 1, \dots, \tau$ **do**

4: Compute gradients and update the original model:

5:
$$\text{grad}^{(t)} = \frac{1}{b} \nabla_{\theta} \sum_{x \in B_*^{(t)}} \ell(x; \theta^{(t)}); \quad \theta^{(t)} = \theta^{(t-1)} - \text{step_size} \cdot \text{grad}^{(t)}.$$

6: Randomly split $D = D_1^{(t)} \cup \dots \cup D_{\kappa}^{(t)}$ that satisfy Eqs. (5) and (6).

7: **for** $k = 1, \dots, \kappa$ **do**

8: Randomly select subset D_{sub} from $D \setminus D_k^{(t)}$.

9: Randomly select μ mini-batches with size b from D_{sub} : $B_1^{(k,t)}, \dots, B_{\mu}^{(k,t)}$.

10: Choose the best mini-batch to approximate the gradient:

11:
$$m_*^{(k,t)} = \arg \min_{m \in [\mu]} \left\| \frac{1}{b} \nabla_{\theta} \sum_{x \in B_m^{(k,t)}} \ell(x; \theta^{(t)}) - \text{grad}^{(t)} \right\|_2^2.$$

12: **for** $x_i \in D_k^{(t)}$ **do**

13: **if** $x_i \in B_*^{(t)}$ **then**

14: $B_{\text{forge}}^{(t)}(x_i) = B_{m_*^{(k,t)}}^{(k,t)}$;

15: **else**

16: $B_{\text{forge}}^{(t)}(x_i) = B_*^{(t)}$.

17: **end if**

18: **end for**

19: **end for**

20: **end for**

21: **Return:** original model $\theta_* = \theta^{(\tau)}$; all forged mini-batches $\{B_{\text{forge}}^{(t)}(x_i) : i \in [n], t \in [\tau]\}$.

- **Sampling Approximation.** Instead of generating a PoR for all data points, we do it for a subset of data points randomly selected from the training dataset D .

- **Combination Approximation.** As discussed in Section III-A (Key Idea 2), we re-use the same PoR for λ data points at a time for the entire training dataset.

In the sampling approximation setting, for both MNIST and CIFAR-10, we use a random subset of $n = 10\text{K}$ data points with $\tau = 2\text{K}$ and $\lambda = 1$.

In the combination approximation setting, we use the entire training dataset of size $n = 60\text{K}$ with $\tau = 12\text{K}$ and $\lambda \in \{10, 100\}$ for MNIST. For CIFAR-10, we use the entire training dataset of size $n = 50\text{K}$ with $T = 10\text{K}$ and $\lambda = 10$. More details are presented in Appendix C.

MI attacks. We evaluate the following MI attacks:

- *EnhancedMIA* [61] is currently the state-of-the-art MI attack which uses a likelihood ratio test approximately comparing the loss of the target with a threshold.

- *LiRA* [11] is one of the most recent MI attacks with a special focus on low false positive rate for the MI predictions. It performs a likelihood ratio test for the loss of x^* between the distributions of losses from shadow models trained with and without x^* .

- *Xent* [63] is an entropy-based MI attack, which computes the cross entropy of the target model output at x^* , and then compares to a label-specific threshold derived from a shadow model.

- *MEntr* [54] is an improved MI attack of Xent, which takes into consideration of correct and wrong classification results when computing the entropy of the target model output at x^* .

- *MIDA* [65] is an MI attack designed for models trained with data augmentation. It classifies sets of augmented samples instead of a single sample by extracting features from losses of the target model output at x^* after data augmentation. Since we use data augmentation only for CIFAR-10, we evaluate MIDA only on this dataset.

The training details including shadow models and threshold selection methods are presented in Appendix C.

Metrics. We use the following three metrics for our evaluation.

To evaluate in Condition 1, we use the L_2 -distance metric precisely defined as follows. Let $M_{\theta_{-i}}$ represent the forged model corresponding to the target of the PoR $x^* = x_i, i \in [n]$. The first metric is the ℓ_2 distance between the parameters of the original model, θ_* , and forged model, θ_{-i} . We report the mean value for $d_\theta = \|\theta_* - \theta_{-i}\|_2^2 / \dim(\theta_*)$.

To evaluate the second condition, we look at the following two metrics. First, is the *membership prediction difference* metric. Let U be the set of data points we want to carry out the MI attack on. Recall that $M_{\theta_{-i}}$ is the forged model used for constructing a PoR for the data point $x_i, i \in [n]$. The metric counts the number of data points in the training dataset D for which the MI attack results in different predictions for at least one of the samples in U for the original and the forged models: $c_{\mathcal{A}}^U = \text{Percentage of data points satisfying } |\{x_i \in D \mid \exists z \in U \text{ s. t. } \mathcal{A}(z, M_{\theta_*}, \psi) \neq \mathcal{A}(z, M_{\theta_{-i}}, \psi)\}|$. To better understand where the MI predictions differ, for each pair of models $\{M_{\theta_*}, M_{\theta_{-i}}\}$ we consider the following three cases separately: (1) In the first case, we look at the MI attack’s predictions for the target data point. Note that x_i is a member of original model M_{θ_*} but a non-member of the forged model, $M_{\theta_{-i}}$. We refer to it as the `Diff` setting. (2) The second case corresponds to data points that are *common* to both the models, i.e., $D_{-i} = D \setminus \{x_i\}$. We refer to this as the `Common` setting. Due to our constraint of academic resources, we perform the following approximation. Instead of testing on the entire $n - 1$ data points in D_{-i} , we choose a subset of 5 data points sampled at random for each $i \in [n]$. (3) In the third case, we carry the MI attacks on data points of the validation dataset which are non-members for both the models. Due to our constraint of academic resources, we again carry out the test on a subset of 5 sampled at random for each $i \in [n]$. We refer to this as the `Validation` setting. More details are presented in Appendix C.

The final metric is the *membership score difference* metric which measures the change in the prediction scores of the MI attack between the forged and original models: $s_{\mathcal{A}} = |\mathcal{A}.\text{score}(x_i, M_{\theta_{-i}}, \psi) - \mathcal{A}.\text{score}(x_i, M_{\theta_*}, \psi)|$.

B. Quality of Forged PoLs

In this section, we answer Q1. For this, we look at the two conditions for generating a valid PoR as discussed above.

For evaluating Condition 1, we report the L_2 -distance metric d_θ in Fig. 3. We observe that the forged models are very close to the original models for all of our experimental settings. Additionally, we observe that the distance increases for $\lambda = 10$. This is because it is now more difficult to find forged mini-batches that approximate the original gradients well. Thus, the parameter λ trades-off the computational overhead of generating a PoR with its quality.

Next, we discuss our evaluation of Condition 2. We start by analyzing the membership prediction difference metric in the `Diff` setting (Table I). If the MI attack were perfect, then the metric would have a value of 100%. On the other hand, if forging were perfect, then the metric would have a value of 0%. Our empirical results show that the forging works quite well - the MI predictions differ only for at most 0.3% and 12.4% (Xent attack on VGG-mini with $n = 50K^\dagger$, $\lambda = 10$ and $\kappa = 2$) of all the data points in MNIST and CIFAR-10, respectively.

For the `Common` setting (Table II), if the MI attack were perfect, the metric would have a value of 0%. This is because the data points in D_{-i} are members of *both* the models $\{M_{\theta_*}, M_{\theta_{-i}}\}$. Forging does not affect the data points in D_{-i} and hence, ideally we expect the metric to be 0%. Here, a disagreement on the prediction is an indication of a false negative error on *one* of the models. We observe that the MI attacks have different predictions for at most 1.2% and 11.08% of the data points for MNIST and CIFAR-10, respectively. It is important to note that the LiRA and EnhancedMIA attacks have a much lower prediction difference - 0.011% and 0.35% for MNIST and CIFAR-10, respectively. This is because they are currently the state-of-the-art attacks that are designed to maximize prediction accuracy under a *low* false positive rate to improve the reliability of MI attacks (see our discussion in Section IV-E). Corollarily, the quality of the forging is significantly better under these state-of-the-art attacks.

Finally for the `Validation` setting (Table III), the metric would again have a value of 0% under a perfect MI attack. This is because the data points in the validation dataset are *not* members for both the models. Additionally, since forging is completely agnostic of these data points, we again expect a value of 0% ideally. A difference in the two predictions here means that the MI attack has a false positive error on one of the models. We observe that MI attacks have different predictions for 0.347% and 11.3% of the data points for MNIST and CIFAR-10, respectively. Similar to above, the prediction difference is lower (consequently, the quality of forging is better) for LiRA and EnhancedMIA attacks - 0.111% and 6.336% for MNIST and CIFAR-10, respectively.

In addition to the difference in the prediction bits, we also evaluate the membership score difference metric, $s_{\mathcal{A}}$, for completeness. For MNIST (Fig. 4), $s_{\mathcal{A}}$ is almost close to zero for all the MI attacks. For CIFAR-10 (Fig. 4), $s_{\mathcal{A}}$ is close to zero for most of the data points but with a slightly higher variance. This is expected since the models for CIFAR-10 are much larger and more complex than MNIST. Additional results are presented in Appendix C.

C. Impact of Hyper-parameters

In this section, we answer Q2. Specifically, we analyze the impact of the two key hyper-parameters of our proposed Algorithm 2, number of splits κ and number of candidate mini-

Dataset	Model	n	λ	κ	% Data points with different MI predictions in the <code>Diff</code> setting				
					LiRA [12]	EnhancedMIA [62]	MEntr [54]	Xent [63]	MIDA [65]
MNIST	LeNet5	10K	1	5	0.00%	0.01%	0.14%	0.25%	-
		60K	10	5	0.03%	0.09%	0.32%	0.31%	-
		60K	100	5	0.08%	0.57%	1.31%	1.30%	-
CIFAR-10	ResNet-mini	10K	1	2	0.63%	5.46%	2.50%	5.26%	2.39%
		50K	10	2	0.46%	2.16%	3.20%	4.69%	2.97%
		50K [†]	10	2	0.42%	4.30%	8.42%	8.51%	6.05%
	VGG-mini	10K	1	2	0.52%	4.45%	3.71%	3.75%	1.45%
		50K	10	2	0.36%	3.68%	7.10%	7.14%	7.26%
		50K [†]	10	2	0.34%	3.63%	3.53%	12.4%	7.30%

TABLE I: Membership prediction differences ($c_{\mathcal{A}}^U$) in the `Diff` setting. [†] means the modified SGD is used.

Dataset	Model	n	λ	κ	% Data points with different MI predictions in the <code>Common</code> setting				
					LiRA [12]	EnhancedMIA [62]	MEntr [54]	Xent [63]	MIDA [65]
MNIST	LeNet5	10K	1	5	0.00%	0.02%	0.04%	0.06%	-
		60K	10	5	0.01%	0.10%	0.30%	0.26%	-
		60K	100	5	0.06%	0.57%	1.33%	1.18%	-
CIFAR-10	ResNet-mini	10K	1	2	0.04%	6.29%	2.47%	2.11%	1.04%
		50K	10	2	0.23%	2.15%	3.26%	4.85%	3.11%
		50K [†]	10	2	0.35%	4.31%	8.57%	8.62%	6.21%
	VGG-mini	10K	1	2	0.00%	4.69%	3.80%	3.47%	1.05%
		50K	10	2	0.07%	3.81%	7.54%	7.59%	7.61%
		50K [†]	10	2	0.22%	3.59%	3.65%	11.1%	6.85%

TABLE II: Membership prediction differences ($c_{\mathcal{A}}^U$) in the `Common` setting. [†] means the modified SGD is used.

Dataset	Model	n	λ	κ	% Data points with different predictions in the <code>Validation</code> setting				
					LiRA [12]	EnhancedMIA [62]	MEntr [54]	Xent [63]	MIDA [65]
MNIST	LeNet5	10K	1	5	0.00%	0.02%	0.07%	0.06%	-
		60K	10	5	0.01%	0.11%	0.35%	0.25%	-
		60K	100	5	0.06%	0.57%	1.31%	1.30%	-
CIFAR-10	ResNet-mini	10K	1	2	0.36%	6.34%	2.15%	5.90%	2.71%
		50K	10	2	0.34%	2.12%	3.35%	4.63%	3.03%
		50K [†]	10	2	0.31%	4.34%	7.52%	7.64%	5.89%
	VGG-mini	10K	1	2	0.19%	4.71%	1.97%	2.16%	1.29%
		50K	10	2	0.20%	3.77%	6.31%	6.32%	6.61%
		50K [†]	10	2	0.23%	3.58%	3.55%	11.3%	6.95%

TABLE III: Membership prediction differences ($c_{\mathcal{A}}^U$) in the `Validation` setting. [†] means that modified SGD is used.

Dataset	Model	n	λ	κ	ℓ_1 distance
MNIST	LeNet5	10k	1	5	0.0077 ± 0.0001
		60k	10	5	0.0249 ± 0.0002
		60k	100	5	0.0941 ± 0.0005
CIFAR-10	ResNet-mini	10k	1	2	0.0166 ± 0.0001
		50k	10	2	0.0285 ± 0.0002
		50k [†]	10	2	0.0285 ± 0.0002
	VGG-mini	10k	1	2	0.0166 ± 0.0001
		50k	10	2	0.0285 ± 0.0001
		50k [†]	10	2	0.0285 ± 0.0002

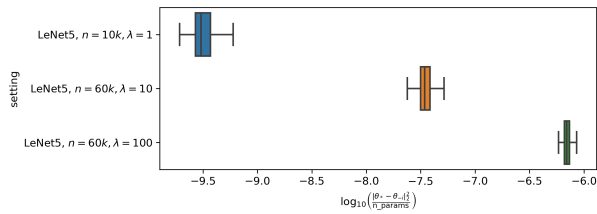
TABLE IV: Uniformity of forged mini-batches measured in ℓ_1 distance between frequencies of all samples and the uniform distribution. Mean and standard errors among 100 PoRs are reported for each setting. The standard SGD yields a distance up to 0.177. Results in all settings are much lower than this value, indicating the forged mini-batches are adequately uniform.

batches μ , on the quality of forging. A large κ leads to low mini-batch re-using and a large μ means more candidate mini-batches to choose from – both come at the cost of increased computational overhead (see Section III-A). We evaluate for $\kappa \in \{5, 10\}$ and $\mu \in \{200, 400\}$ on MNIST. The L_2 -distance metric d_θ is reported in Fig. 6. We observe that increasing

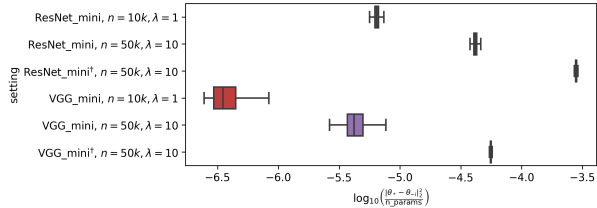
the values of both κ and μ do not show any significant improvement over the values reported originally in Fig. 3a. We report the correspond values for the membership prediction difference metric in the `Diff` setting in Table V. Again we observe that the values are comparable to that of our prior results in Table I for most of our experimental settings. We see a slight improvement for the case of $\lambda = 100$ and $\mu = 400$. This validates our choice of the hyper-parameters for our primary experiments in Section IV-B.

D. Distribution of Forged Mini-batches

In this section, we answer Q3. Stated otherwise, the goal here is to check whether a verifier can distinguish between a forged PoL and a true one (i.e., one recording a true SGD training process). We answer this question from a statistical perspective here – we test whether the distribution of the samples in the forged mini-batches satisfy uniform distribution (which would be the case for a true PoL). Specifically, we compute the ℓ_1 -distance between the frequencies of all the samples in the forged mini-batches $\{B_{\text{forge}}^{(t)}(x_i)\}_{t=1}^T$ and the uniform distribution (Table IV). We choose this as our metric because



(a) MNIST.



(b) CIFAR-10 († means the modified SGD is used)

Fig. 3: Box plots of L_2 model distances (d_θ) in the log scale: $\log_{10}(\|\theta_* - \theta_{-i}\|_2^2 / \dim(\theta_*))$. Smaller values indicate the forged models are closer to the original model.

standard statistical tests, such as the Kolmogorov–Smirnov test, are a misfit for our setting (see Appendix C for details). We observe that ℓ_1 -distances in all of our experimental settings have a very low value indicating high uniformity in the distributions. As expected, a larger λ results in less uniformity. Additionally, the uniformity of the modified SGD setting is similar to that of the standard SGD setting.

E. Discussion

The key takeaways from our evaluation are as follows.

First, we are able to generate a valid PoR for most of the data points. Based on the above observations, we can conclude that we are able to generate membership inference equivalent³ models (Definition 5) for at least 98.8% and 87.8% of the data points of MNIST and CIFAR-10, respectively. In other words, we are able to generate a valid PoR for the same number of data points. Thus, we see that our PoR generation algorithm performs remarkably well in practice even for a complex dataset as CIFAR-10.

Second, our performance is even better on the state-of-the-art MI attacks that focus on a low false positive regime. The reason why this is an important observation is that there is a growing consensus that, for improving the practical reliability of membership inferencing predictions, average accuracy is not a meaningful metric for evaluating MI attacks [12], [44], [59], [62]. Rather, a better metric is measuring the true positive rate of an MI attack under *low* false positive rate conditions. Out of the four evaluated attacks, only the more recent LiRA and EnhancedMIA attacks are currently successful in the low false positive rate regime (LiRA has $10\times$ better performance

³modulo our computation relaxation of testing only on a random sample of D_{-i}

than the other two attacks as reported in [12]). Our proposed algorithm performs even better on these two attacks – we are able to generate a valid PoR for 99.9% and 95.7% of the data points of MNIST and CIFAR-10, respectively.

Third, the λ parameter (the number of data points that share the *same* PoR– combination approximation) results in a computational cost/quality of generated PoR trade-off. Lower the value of λ , better is the quality of the generated PoR at the cost of increased computational overhead. Specifically, the quality of the forging (equivalently, the generated PoRs) is the best for $\lambda = 1$ which is studied under the sampling approximation evaluation setting.

V. IMPLICATIONS OF A PoR

In this section, we discuss the implications of a PoR in the context of MI attacks.

Consequences for the model owner. The primary consequence of our ability to construct valid PoRs is that it establishes the unreliability of MI attacks in practice. Using a PoR, the model owner can discredit any membership inference claim from an adversary on the data points of its training dataset. As a result, the adversary fails to bring any real consequences for the model owner based on its prediction. For instance, say an adversary presents its membership inference claim on a data point x^* in a court of law. However, as discussed above, a valid PoR enables the model owner to plausibly deny the MI prediction and present a counter claim that x^* is in fact *not* a member. This is enough to raise a reasonable doubt on the adversary’s claim. The model owner can, thus, get the case to be dismissed, thereby relieving themselves of any legal consequence. Thus, an adversary cannot “go-to-court” with a membership inference claim. Consequently, PoRs bring to question the viability and severity of any real threat a model owner faces from an MI attack in practice.

It is interesting to note that in some real-world settings, the model owner’s ability to generate valid PoRs could have adverse implications. For instance, consider a setting where an auditor wants to check whether a model used a target data point for its training without proper legal consent. This could be useful for detecting various instances of data misuse, such as privacy violation, copyright abuse or jurisdictional infringement. The auditor can launch a MI attack on the model for the target data point and register a case in a court of law based on the prediction. However, as discussed above, the model owner can successfully repudiate the auditor’s claim with a PoR and get the case to be acquitted. It is interesting to note that although the entity carrying out the attack is designated as the “adversary” in our technical formalization, the actual semantics could be quite different in reality. In the aforementioned case, the challenger (model owner) is the unscrupulous entity who can now get away with data misuse.

Re-evaluating our understanding of MI attack predictions. MI attacks predictions cannot be relied upon for data points with a valid PoR in practice. However, as discussed in Section

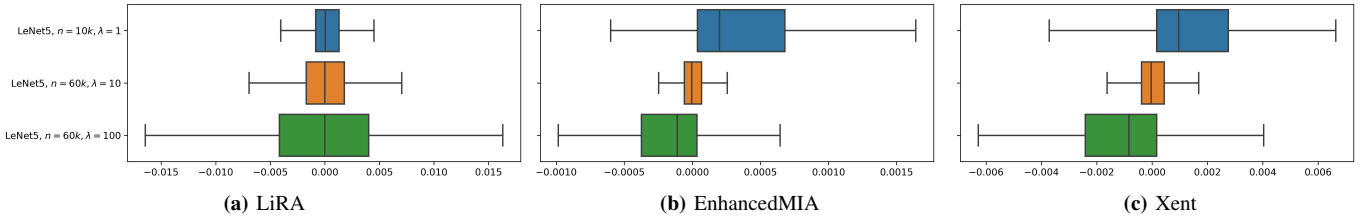


Fig. 4: Box plots of membership score differences (s_A) on MNIST. Most score differences are close to zero, indicating these MI attacks output similar scores between original and forged models.

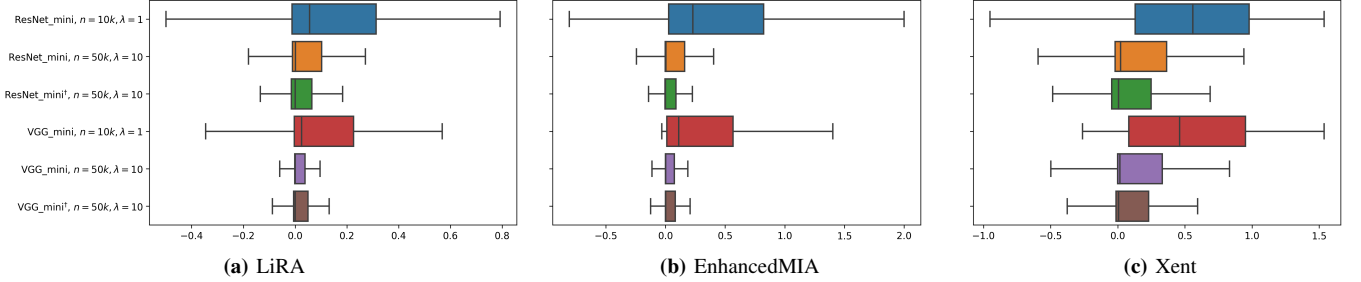


Fig. 5: Box plots of membership score differences (s_A) on CIFAR10 († means the modified SGD is used). Most score differences are close to zero, indicating these MI attacks output similar scores between original and forged models. The values and variances are higher than those in MNIST experiments, which is likely because models for CIFAR10 are larger and more complex. There is no significant difference between ResNet and VGG networks.

n	λ	κ	μ	% Data points with different predictions in the <i>Diff</i> setting			
				LiRA	EnhancedMIA	MEntr	Xent
10k	1	10	200	0.00%	0.01%	0.14%	0.27%
60k	10	10	200	0.02%	0.13%	0.31%	0.31%
60k	100	10	200	0.07%	0.65%	1.39%	1.30%
60k	100	5	400	0.08%	0.56%	1.35%	1.27%

TABLE V: Membership prediction differences in the *Diff* setting on MNIST, with different κ and μ values compared to Table I (where $\kappa = 5$ and $\mu = 200$). There is a slight or no improvement on PoR failure rates when increasing κ from 5 to 10 or μ from 200 to 400.

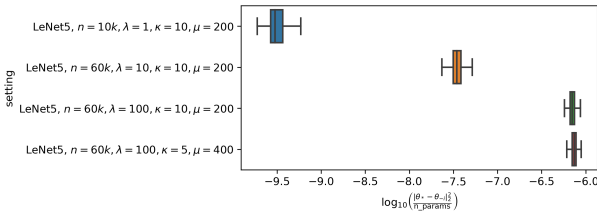


Fig. 6: Box plot of L_2 model distances on MNIST, with different κ and μ values compared to Fig. 3a (where $\kappa = 5$ and $\mu = 200$). There is no improvement on model distances when increasing κ from 5 to 10 or μ from 200 to 400.

III-B, we observe that it is impossible to generate a valid PoR for all possible data points. Specifically, one cannot generate a valid PoR for outliers or out-of-distribution (OOD) data points. This is also highlighted in our empirical evaluation (Section IV). Based on the above observation, we argue that our current understanding of the *practical implications* of an MI attack predictions requires re-evaluation. We argue that a MI attack is perhaps better suited for distinguishing between in-liear/in-distribution and outlier/out-of-distribution data points

in practice. This highlights the disparity in privacy vulnerability of the different data points – while the practical efficacy of an MI attack on in-distribution data points is questionable, data points that are not well-represented in the dataset (such as, data points from individuals belonging to minority groups) are still susceptible to privacy violations.

Similar observations have been made in prior literature as well. Carlini et al. [12] observed that MI attacks are able to identify out-of-distribution data points (records) with higher success. Ye et al. [62] also observed that different data points have different vulnerabilities. Watson et al. [59] showed that the success of an MI attack is correlated with the model’s difficulty of correctly classifying a target sample – well-represented points have higher false positive rates. A concurrent work [44] shows that the membership score distributions of member samples are similar to that of their non-member neighbors and argues that MI attacks identify the memorized sub-populations (samples that are close in the latent space) and not the individual samples (records). In other words, MI attacks can identify that a sample from a sub-population is a member, but they cannot reliably identify which exact sample in that sub-population is in the training dataset.

Re-evaluating the privacy leakage of ML models. Conceptually for an ML attack, the sensitive information in contention is the single bit indicating the data point’s membership status. However, a PoR empowers the model owner to plausibly deny any claims on this membership status. This highlights the limitations of ML attacks for measuring privacy leakage of ML models in practice. For instance, in the real-world setting of a privacy audit discussed in the above paragraph, ML attacks clearly fail to capture the correct privacy semantics. It is important to note that the validity of a PoR is completely agnostic of the ML attack, i.e., a PoR is effective even if the ML attack makes genuinely reliable predictions (for instance, with very low false positive rate on the entire input distribution). In other words, inferring just the membership status is inadequate to make any definitive conclusions about a model’s privacy leakage in many real-world settings. This urges us to re-evaluate the rationale behind using ML attacks as a privacy metric in practice.

VI. DISCUSSION

In this section, we discuss several points relevant to PoRs.

Zero-knowledge access to PoRs. It is important to note that revealing a PoR in the clear to an adversary could be counterproductive for privacy. This is because the PoR records all the true data points in $D \setminus \{x^*\}$ (in the form of the recorded mini-batches) which is revealed to the adversary, thereby violating privacy. So in practice, the adversary should be allowed a *zero-knowledge* access to the PoR. By this statement we mean that the adversary should be convinced of the validity of the PoR *without* learning anything else about the rest of the data points of the dataset. Note that this is not a problem in the context of machine unlearning (for forgeability, Section I-D) or establishing model ownership (for PoLs, Section I-C). However, privacy is innate in the context of ML attacks. We list down a few mitigation strategies for the model owner as follows:

- 1) The model owner can use zero-knowledge proofs and achieve this goal cryptographically. Specifically, the model owner can first prove via private set intersection [] that $D' \cap \{x^*\} = \emptyset$. Next, they can commit to D' and show via zero-knowledge proofs that the computation of the training log was performed correctly on D' .
- 2) The verification of the PoR log can be performed by a trusted third-party entity. For instance, as mentioned in Section V, regulatory bodies such as the Electronic Frontier Foundation (EFF) or a judge/juror in the court of law could act as the verifier. The privacy of the data points used in the PoR is thereby protected via legal obligations.
- 3) The PoR can be constructed from a public dataset, D_p , instead of from $D \setminus \{x^*\}$, such that D_p is drawn from the distribution as D . The assumption of having a public dataset is common in both ML [60], [9], [31] as well as privacy literature [36], [5], [6], [45]. The dataset can

be small and obtained by manual labeling [37]. Recall, that for generating a PoR from $D' = D \setminus \{x^*\}$, all the original mini-batches $B^{(t)}, t \in [\tau]$ that contain the data point x^* are replaced with forged ones, $B_{\text{forge}}^{(t)}$, without x^* . In order to construct the PoR from the public dataset, D_p , we need to replace *all* the τ original mini-batches with forged mini-batches sampled from D_p . Note that generating a PoR from D_p would potentially degrade its quality, i.e., the resulting tolerance parameter $\|\theta - \theta'\|_2$ would be higher. This is because first, the mini-batches for every iteration has to be replaced, and second, none of the forged mini-batches contain any of the data points in D resulting in a poorer approximation of the original gradient.

Knowledge about the size of the dataset In our context, an additional assumption is that the the adversary cannot know the exact size of the dataset. It is so because with the current mechanism, the PoR can be only constructed from $D' \subset D$, i.e., a dataset that is strictly smaller than $|D| = n$. In case the adversary already knows n , then they can “reject” the PoR just based on the dataset size.

Spoofing attacks on PoL. Recall that PoL was originally introduced in the context of establishing model ownership – the central idea being only an entity who has performed the training from scratch (or has expended at least the equivalent computational effort) should be able to produce a valid PoL. However, recent work [18], [67] has shown that it is in fact possible for an adversary to *spoof* a PoL for a model they did train with less much less computational effort than the actual model owner (trainer). This highlights the limitations of using PoL for resolving model ownership. However, the existence of such spoofing attacks have no bearing in our context. It is because for a PoR to be valid, it is enough to just establish computational feasibility to have obtained M'_θ from D' . In other words, the fact that it is plausible to have trained M'_θ on D' is enough to raise a reasonable doubt on the adversary’s membership inference claim on the data point x^* . Hence, even if the challenger “spoofs” the PoL (hence PoR) it does not affect our claim of repudiation – the mechanism of generation of the PoR is completely irrelevant to our goal of establishing computational feasibility. As discussed in Section V, in a court-of-law, the burden-of-proof would lie on the adversary, i.e., establishing *beyond* a reasonable doubt that was x^* indeed used by the challenger for training.

PoR for a claim on non-membership. In this paper, we explore the question of repudiating a membership claim, i.e., if $x \in D$. However, a complementary question could be when an adversary claims that a data point x is *not* a member, $x^* \notin D$. A real-world example of such a scenario could be when an adversary wants to claim that the model owner has intentionally excluded some data points, say that belong to the minority population, to bias the training model. In this case, a PoR would have to show that the model owner could have obtained M'_θ from the dataset $D' = D \cup \{x^*\}$. Given

VII. RELATED WORK

a PoL for the $\langle M_\theta, D \rangle$, we outline a possible strategy for the construction of such a PoR. First, select a set of random iterations $H \subset [\tau]$. Next, the original mini-batch $B^{(t)}$ for each iteration in $t \in H$ is replaced with a forged mini-batch $B_{\text{forge}}^{(t)}$ such that $x^* \in B_{\text{forge}}^{(t)}$. We surmise that as long as x^* is not an outlier, the above strategy would generate a valid PoR. We leave a more detailed exploration of such a PoR as a part of future work.

Roles of the challenger and adversary. Recall that a PoR is essentially a forged PoL. Thus, we leverage forgeability, a concept introduced in the context of machine unlearning, to repudiate claims on membership inferencing. Despite relying on the same technical tool (forged PoLs) the roles of the challenger and adversary are essayed by different parties in the two contexts.

First, we discuss the forging security game.

Definition 6 (Forging Security Game $\mathcal{G}_F(\cdot)$). The forging security game $\mathcal{G}_F(\cdot)$ is defined as follows:

- 1) Adversary \mathcal{A} has a dataset D and a model M_θ trained on it.
- 2) Challenger \mathcal{C} selects a point $x_- \in D$ to be deleted and sends it to the adversary \mathcal{A} .
- 3) Adversary \mathcal{A} provides a *forged* PoL based on Algorithm 1
- 4) Challenger \mathcal{C} verifies the PoL.

For the context of machine unlearning, the challenger has to be somebody who knows a data point in D (in practice, it is typically an individual who has contributed to D). On the other hand, the model owner is actually the adversary who is trying to be unscrupulous with a deletion request. Thus using the above attack, the model owner can *claim* to have unlearned for free.

Now, let's look at the PoR security game.

Definition 7 (PoR Security Game, $\mathcal{G}_{\text{PoR}}(\cdot)$). The PoR security game is defined as follows:

- 1) Challenger \mathcal{C} holds a private dataset D and a model M_θ trained on it. The model is publicly released.
- 2) Adversary \mathcal{A} *correctly* predicts that a data point $x^* \in D$, i.e., $\mathcal{A}(x^*, M_\theta, \Psi) = 1$, and sends this membership inferencing claim to the challenger \mathcal{C} .
- 3) Challenger \mathcal{C} responds with a Proof-of-Repudiation, PoR.
- 4) Adversary \mathcal{A} verifies the PoR.

As discussed in Section I-B, in this paper we focus on ML attacks in practice. Hence, for a membership inferencing, the model owner is the challenger who is trying to fend themselves from an adversary carrying out an ML attack. Thus, the role of the model owner is switched in the two contexts.

Membership inference attacks predict whether a particular data point was used for training a model ([23], [47], [17], [16], [52], [13], [39], [55], [11], [14], [62]). There is a connection between membership inferencing and other topics in ML privacy, such as differential privacy ([13], [26], [24], [41]), memorization ([19], [66]), and over-fitting ([64]).

Machine unlearning is the task to delete a data point from a learned model and approximate machine unlearning outputs a model that is statistically indistinguishable from the model obtained by deleting and retraining ([10], [20], [21], [48], [7], [58], [42], [49], [25], [32]). The recently proposed forging attack in [57] challenges the foundation of machine unlearning by generating a forged PoL log which is indistinguishable from the correct one (dataset after deleting). In this paper, we have showed a connection between membership inference attacks and forging attacks.

Concurrent work by Rezaei et al. [44] has also studied the practical unreliability of ML attacks. However, their approach is completely different from our concept of PoRs. They consider an auditing scenario where an auditor carries out an ML attack that claims to have a low false positive rate. Given a list of data points that the attack claimed as members, the auditee (model owner) crafts a "discrediting dataset" consisting of non-members data points that are mis-predicted by the ML attack as members (false positive error). This challenges the reliability of the ML predictions.

It is important to note that there is a fundamental difference between prior literature on defenses against ML attacks [46], [40], [50], [30] and our setting. Defenses are designed to reduce the efficacy (success rate) of ML attacks. The key insight is to induce similar model output distribution on both the training (member) and testing (non-member) dataset and is achieved via either training time techniques (such as dropout [46], ℓ_2 -norm regularization [52], model stacking [56], min-max adversary regularization [40], differential privacy [27], [4], early stopping [54], knowledge distillation [50]) and or inference time mechanisms (such as output perturbation [30]). However, our setting is completely different – a PoR enables a model owner to discredit a membership inference claim *post-attack*. The generation of a PoR requires *no* modifications for pre-computing the forged mini-batches only to reduce computational cost of generating the PoRs for all the data points in D . to the model's training or inference pipeline. In other words, a PoR makes an ML attack ineffective in practice even against a ML model that has been already trained or is publicly available.

VIII. CONCLUSION

In this paper, we investigate the reliability of membership inference in practice. Specifically, we study if it is possible for a model owner to refute a membership inference claim by introducing the notion of Proof-of-Repudiation (PoR). A

PoR enables a model owner to plausibly deny the membership inference prediction and discredit the predictions of an MI attack. Consequently, an adversary cannot “go-to-court” with the prediction of an MI attack. The concrete construction is based on the concept of forgeability introduced by Thudi et al. [57]. Our empirical evaluations have shown that it is possible to construct valid PoRs efficiently in practice.

Acknowledgements. This material is partially based upon work supported by the National Science Foundation under Grant # 2127309 to the Computing Research Association for the CIFellows Project. Kamalika Chaudhuri and Zhifeng Kong would like to thank NSF under CNS 1804829, ONR under N00014-20-1-2334 and ARO MURI W911NF2110317 for research support.

REFERENCES

- [1] General data protection regulation gdpr. <https://gdpr-info.eu/>, 2016.
- [2] California consumer privacy act (ccpa). <https://oag.ca.gov/privacy/ccpa>, 2018.
- [3] Introducing a new privacy testing library in tensorflow. <https://blog.tensorflow.org/2020/06/introducing-new-privacy-testing-library.html>, 2020.
- [4] Martin Abadi, Andy Chu, Ian Goodfellow, H. Brendan McMahan, Ilya Mironov, Kunal Talwar, and Li Zhang. Deep learning with differential privacy. In *Proceedings of the 2016 ACM SIGSAC Conference on Computer and Communications Security, CCS '16*, page 308–318, New York, NY, USA, 2016. Association for Computing Machinery.
- [5] Raef Bassily, Albert Cheu, Shay Moran, Aleksandar Nikolov, Jonathan Ullman, and Zhiwei Steven Wu. Private query release assisted by public data. In *ICML*, 2020.
- [6] Amos Beimel, Aleksandra Korolova, Kobbi Nissim, Or Sheffet, and Uri Stemmer. The power of synergy in differential privacy: Combining a small curator with local randomizers. In *ITC*, 2020.
- [7] Michele Borassi, Alessandro Epasto, Silvio Lattanzi, Sergei Vassilvitskii, and Morteza Zadimoghaddam. Sliding window algorithms for k-clustering problems. *Advances in Neural Information Processing Systems*, 33:8716–8727, 2020.
- [8] Lucas Bourtole, Varun Chandrasekaran, Christopher A. Choquette-Choo, Hengrui Jia, Adelin Travers, Baiwu Zhang, David Lie, and Nicolas Papernot. Machine unlearning. In *2021 IEEE Symposium on Security and Privacy (SP)*, pages 141–159, 2021.
- [9] Xiaoyu Cao, Minghong Fang, Jia Liu, and Neil Zhenqiang Gong. Fltrust: Byzantine-robust federated learning via trust bootstrapping. 2021.
- [10] Yinzhi Cao and Junfeng Yang. Towards making systems forget with machine unlearning. In *2015 IEEE Symposium on Security and Privacy*, pages 463–480. IEEE, 2015.
- [11] Nicholas Carlini, Steve Chien, Milad Nasr, Shuang Song, Andreas Terzis, and Florian Tramer. Membership inference attacks from first principles. *arXiv preprint arXiv:2112.03570*, 2021.
- [12] Nicholas Carlini, Steve Chien, Milad Nasr, Shuang Song, Andreas Terzis, and Florian Tramer. Membership inference attacks from first principles, 2021.
- [13] Nicholas Carlini, Chang Liu, Úlfar Erlingsson, Jernej Kos, and Dawn Song. The secret sharer: Evaluating and testing unintended memorization in neural networks. In *28th USENIX Security Symposium (USENIX Security 19)*, pages 267–284, 2019.
- [14] Nicholas Carlini, Florian Tramer, Eric Wallace, Matthew Jagielski, Ariel Herbert-Voss, Katherine Lee, Adam Roberts, Tom Brown, Dawn Song, Úlfar Erlingsson, et al. Extracting training data from large language models. In *30th USENIX Security Symposium (USENIX Security 21)*, pages 2633–2650, 2021.
- [15] Kamalika Chaudhuri, Jacob Imola, and Ashwin Machanavajjhala. Capacity bounded differential privacy. In H. Wallach, H. Larochelle, A. Beygelzimer, F. d’Alché-Buc, E. Fox, and R. Garnett, editors, *Advances in Neural Information Processing Systems*, volume 32. Curran Associates, Inc., 2019.
- [16] Cynthia Dwork, Adam Smith, Thomas Steinke, and Jonathan Ullman. Exposed! a survey of attacks on private data. *Annu. Rev. Stat. Appl.*, 4(1):61–84, 2017.
- [17] Cynthia Dwork, Adam Smith, Thomas Steinke, Jonathan Ullman, and Salil Vadhan. Robust traceability from trace amounts. In *2015 IEEE 56th Annual Symposium on Foundations of Computer Science*, pages 650–669. IEEE, 2015.
- [18] Congyu Fang, Hengrui Jia, Anvith Thudi, Mohammad Yaghini, Christopher A. Choquette-Choo, Natalie Dullerud, Varun Chandrasekaran, and Nicolas Papernot. On the fundamental limits of formally (dis)proving robustness in proof-of-learning, 2022.
- [19] Vitaly Feldman. Does learning require memorization? a short tale about a long tail. In *Proceedings of the 52nd Annual ACM SIGACT Symposium on Theory of Computing*, pages 954–959, 2020.
- [20] Antonio Ginart, Melody Guan, Gregory Valiant, and James Y Zou. Making ai forget you: Data deletion in machine learning. *Advances in Neural Information Processing Systems*, 32, 2019.
- [21] Chuan Guo, Tom Goldstein, Awni Hannun, and Laurens Van Der Maaten. Certified data removal from machine learning models. *arXiv preprint arXiv:1911.03030*, 2019.
- [22] Kaiming He, Xiangyu Zhang, Shaoqing Ren, and Jian Sun. Deep residual learning for image recognition. In *Proceedings of the IEEE Conference on Computer Vision and Pattern Recognition (CVPR)*, June 2016.
- [23] Nils Homer, Szabolcs Szelinger, Margot Redman, David Duggan, Waibhav Tembe, Jill Muehling, John V Pearson, Dietrich A Stephan, Stanley F Nelson, and David W Craig. Resolving individuals contributing trace amounts of dna to highly complex mixtures using high-density snp genotyping microarrays. *PLoS genetics*, 4(8):e1000167, 2008.
- [24] Thomas Humphries, Matthew Rafuse, Lindsey Tulloch, Simon Oya, Ian Goldberg, Urs Hengartner, and Florian Kerschbaum. Differentially private learning does not bound membership inference. *arXiv preprint arXiv:2010.12112*, 2020.
- [25] Zachary Izzo, Mary Anne Smart, Kamalika Chaudhuri, and James Zou. Approximate data deletion from machine learning models. In *International Conference on Artificial Intelligence and Statistics*, pages 2008–2016. PMLR, 2021.
- [26] Matthew Jagielski, Jonathan Ullman, and Alina Oprea. Auditing differentially private machine learning: How private is private sgd? *Advances in Neural Information Processing Systems*, 33:22205–22216, 2020.
- [27] Bargav Jayaraman and David Evans. Evaluating differentially private machine learning in practice. In *Proceedings of the 28th USENIX Conference on Security Symposium, SEC’19*, page 1895–1912, USA, 2019. USENIX Association.
- [28] Bargav Jayaraman, Lingxiao Wang, Katherine Knipmeyer, Quanquan Gu, and David Evans. Revisiting membership inference under realistic assumptions. *Proceedings on Privacy Enhancing Technologies*, 2021(2):348–368, 2021.
- [29] Hengrui Jia, Mohammad Yaghini, Christopher A. Choquette-Choo, Natalie Dullerud, Anvith Thudi, Varun Chandrasekaran, and Nicolas Papernot. Proof-of-learning: Definitions and practice. In *2021 IEEE Symposium on Security and Privacy (SP)*, pages 1039–1056, 2021.

- [30] Jinyuan Jia, Ahmed Salem, Michael Backes, Yang Zhang, and Neil Zhenqiang Gong. Memguard: Defending against black-box membership inference attacks via adversarial examples. In *Proceedings of the 2019 ACM SIGSAC Conference on Computer and Communications Security*, CCS '19, page 259–274, New York, NY, USA, 2019. Association for Computing Machinery.
- [31] Peter Kairouz, H. Brendan McMahan, Brendan Avent, Aurelien Bellet, Mehdi Bennis, Arjun Nitin Bhagoji, Kallista Bonawitz, Zachary Charles, Graham Cormode, Rachel Cummings, Rafael G.L. D'Oliveira, Hubert Eichner, Salim El Rouayheb, David Evans, Josh Gardner, Zachary Garrett, Adria Gascon, Badih Ghazi, Phillip B. Gibbons, Marco Gruteser, Zaid Harchaoui, Chaoyang He, Lie He, Zhouyuan Huo, Ben Hutchinson, Justin Hsu, Martin Jaggi, Tara Javidi, Gauri Joshi, Mikhail Khodak, Jakub Konecny, Aleksandra Korolova, Farinaz Koushanfar, Sanmi Koyejo, Tancrede Lepoint, Yang Liu, Prateek Mittal, Mehryar Mohri, Richard Nock, Ayfer Ozgur, Rasmus Pagh, Hang Qi, Daniel Ramage, Ramesh Raskar, Mariana Raykova, Dawn Song, Weikang Song, Sebastian U. Stich, Ziteng Sun, Ananda Theertha Suresh, Florian Tramèr, Praneeth Vepakomma, Jianyu Wang, Li Xiong, Zheng Xu, Qiang Yang, Felix X. Yu, Han Yu, and Sen Zhao. Advances and open problems in federated learning. In *arXiv:1912.04977*, 2019.
- [32] Zhifeng Kong and Scott Alfeld. Approximate data deletion in generative models. *arXiv preprint arXiv:2206.14439*, 2022.
- [33] Alex Krizhevsky. The cifar-10 dataset.
- [34] Yann LeCun, Bernhard Boser, John S Denker, Donnie Henderson, Richard E Howard, Wayne Hubbard, and Lawrence D Jackel. Back-propagation applied to handwritten zip code recognition. *Neural computation*, 1(4):541–551, 1989.
- [35] Yann LeCun, Corinna Cortes, and Christopher J.C. Burges. The mnist database of handwritten digits.
- [36] Terrance Liu, Giuseppe Vietri, Thomas Steinke, Jonathan Ullman, and Zhiwei Steven Wu. Leveraging public data for practical private query release, 2021.
- [37] Brendan McMahan and Daniel Ramage. Federated learning: Collaborative machine learning without centralized training data, 2017.
- [38] Sasi Kumar Murakonda and Reza Shokri. ML privacy meter: Aiding regulatory compliance by quantifying the privacy risks of machine learning. *CoRR*, abs/2007.09339, 2020.
- [39] Sasi Kumar Murakonda and Reza Shokri. MI privacy meter: Aiding regulatory compliance by quantifying the privacy risks of machine learning. *arXiv preprint arXiv:2007.09339*, 2020.
- [40] Milad Nasr, Reza Shokri, and Amir Houmansadr. Machine learning with membership privacy using adversarial regularization. In *Proceedings of the 2018 ACM SIGSAC Conference on Computer and Communications Security*, CCS '18, page 634–646, New York, NY, USA, 2018. Association for Computing Machinery.
- [41] Milad Nasr, Shuang Song, Abhradeep Thakurta, Nicolas Papernot, and Nicholas Carlin. Adversary instantiation: Lower bounds for differentially private machine learning. In *2021 IEEE Symposium on Security and Privacy (SP)*, pages 866–882. IEEE, 2021.
- [42] Seth Neel, Aaron Roth, and Saeed Sharifi-Malvajerdi. Descent-to-delete: Gradient-based methods for machine unlearning. In *Algorithmic Learning Theory*, pages 931–962. PMLR, 2021.
- [43] Nicolas Papernot, Patrick McDaniel, Arunesh Sinha, and Michael Wellman. Towards the science of security and privacy in machine learning, 2016.
- [44] Shahbaz Rezaei and Xin Liu. On the discredibility of membership inference attacks, 2022.
- [45] Amrita Roy Chowdhury, Chuan Guo, Somesh Jha, and Laurens van der Maaten. Eiffel: Ensuring integrity for federated learning. In *Proceedings of the 2022 ACM SIGSAC Conference on Computer and Communications Security*, CCS '22, page 2535–2549, New York, NY, USA, 2022. Association for Computing Machinery.
- [46] Ahmed Salem, Yang Zhang, Mathias Humbert, Pascal Berrang, Mario Fritz, and Michael Backes. MI-leaks: Model and data independent membership inference attacks and defenses on machine learning models. *arXiv preprint arXiv:1806.01246*, 2018.
- [47] Sriram Sankararaman, Guillaume Obozinski, Michael I Jordan, and Eran Halperin. Genomic privacy and limits of individual detection in a pool. *Nature genetics*, 41(9):965–967, 2009.
- [48] Sebastian Schelter. "amnesia"-machine learning models that can forget user data very fast. In *CIDR*, 2020.
- [49] Ayush Sekhari, Jayadev Acharya, Gautam Kamath, and Ananda Theertha Suresh. Remember what you want to forget: Algorithms for machine unlearning. *Advances in Neural Information Processing Systems*, 34, 2021.
- [50] Virat Shejwalkar and Amir Houmansadr. Membership privacy for machine learning models through knowledge transfer, 2019.
- [51] Reza Shokri, Marco Stronati, Congzheng Song, and Vitaly Shmatikov. Membership inference attacks against machine learning models. In *2017 IEEE Symposium on Security and Privacy (SP)*, pages 3–18, 2017.
- [52] Reza Shokri, Marco Stronati, Congzheng Song, and Vitaly Shmatikov. Membership inference attacks against machine learning models. In *2017 IEEE symposium on security and privacy (SP)*, pages 3–18. IEEE, 2017.
- [53] Karen Simonyan and Andrew Zisserman. Very deep convolutional networks for large-scale image recognition. *arXiv preprint arXiv:1409.1556*, 2014.
- [54] Liwei Song and Prateek Mittal. Systematic evaluation of privacy risks of machine learning models. In *USENIX Security Symposium*, 2020.
- [55] Shuang Song and David Marn. Introducing a new privacy testing library in tensorflow, 2020.
- [56] Christian Szegedy, Vincent Vanhoucke, Sergey Ioffe, Jon Shlens, and Zbigniew Wojna. Rethinking the inception architecture for computer vision. In *2016 IEEE Conference on Computer Vision and Pattern Recognition (CVPR)*, pages 2818–2826, 2016.
- [57] Anvith Thudi, Hengrui Jia, Iliia Shumailov, and Nicolas Papernot. On the necessity of auditable algorithmic definitions for machine unlearning. In *31st USENIX Security Symposium (USENIX Security 22)*, Boston, MA, August 2022. USENIX Association.
- [58] Enayat Ullah, Tung Mai, Anup Rao, Ryan A Rossi, and Raman Arora. Machine unlearning via algorithmic stability. In *Conference on Learning Theory*, pages 4126–4142. PMLR, 2021.
- [59] Lauren Watson, Chuan Guo, Graham Cormode, and Alexandre Sablayrolles. On the importance of difficulty calibration in membership inference attacks. *ArXiv*, abs/2111.08440, 2021.
- [60] Cong Xie, Oluwasanmi Koyejo, and Indranil Gupta. Zeno++: Robust fully asynchronous SGD. In *Proceedings of the International Conference on Machine Learning*, 2020.
- [61] Jiayuan Ye, Aadyaa Maddi, Sasi Kumar Murakonda, Vincent Bindschadler, and Reza Shokri. Enhanced membership inference attacks against machine learning models. In *Proceedings of the 2022 ACM SIGSAC Conference on Computer and Communications Security*, CCS '22, page 3093–3106, New York, NY, USA, 2022. Association for Computing Machinery.
- [62] Jiayuan Ye, Aadyaa Maddi, Sasi Kumar Murakonda, and Reza Shokri. Enhanced membership inference attacks against machine learning models. *arXiv preprint arXiv:2111.09679*, 2021.
- [63] Samuel Yeom, Irene Giacomelli, Matt Fredrikson, and Somesh Jha. Privacy risk in machine learning: Analyzing the connection to overfitting. *2018 IEEE 31st Computer Security Foundations Symposium (CSF)*, pages 268–282, 2018.
- [64] Samuel Yeom, Irene Giacomelli, Matt Fredrikson, and Somesh Jha. Privacy risk in machine learning: Analyzing the connection to overfitting. In *2018 IEEE 31st computer security foundations symposium (CSF)*, pages 268–282. IEEE, 2018.

- [65] Da Yu, Huishuai Zhang, Wei Chen, Jian Yin, and Tie-Yan Liu. How does data augmentation affect privacy in machine learning? In *Proceedings of the AAAI Conference on Artificial Intelligence*, volume 35, pages 10746–10753, 2021.
- [66] Chiyuan Zhang, Samy Bengio, Moritz Hardt, Benjamin Recht, and Oriol Vinyals. Understanding deep learning (still) requires rethinking generalization. *Communications of the ACM*, 64(3):107–115, 2021.
- [67] Rui Zhang, Jian Liu, Yuan Ding, Zhibo Wang, Qingbiao Wu, and Kui Ren. “adversarial examples” for proof-of-learning. In *2022 IEEE Symposium on Security and Privacy (SP)*, pages 1408–1422, 2022.

APPENDIX

A. Notations

Table VI describes the notations used in the paper.

TABLE VI: Notations used in the paper.

Notation	Meaning
\mathbb{D}	Input data distribution
D	Original Dataset
D'	Forging dataset
\mathcal{A}	Adversary/attack
\mathcal{C}	Challenger
x^*	MI claim made on this point
μ	Number of candidate batches
λ	number of PoRs combined
τ	Number of iterations
M_θ	Original model
M'_θ	Forged model
θ	Parameters of the original model
θ'	Parameters of the forged model
n	Dataset size $ D $
$B^{(t)}$	Original mini-batch for t -th iteration
$B_{\text{forge}}^{(t)}$	Forged mini-batch for t -th iteration
b	Mini-batch size

B. The Complete PoR Generation Algorithm

In Algorithm 3, we present the complete PoR generation algorithm for models trained with the Random Horizontal Flip data augmentation and modified SGD with momentum, weight decay, and learning rate scheduling. For each mini-batch B , we let $\text{Flip}(B) \in \{0,1\}^{|B|}$ be the corresponding binary flag indicating whether each data point has been flipped horizontally at randomly, and $\text{Aug}(\text{Flip}(B), B)$ be the mini-batch after data augmentation.

C. Experimental Configuration and Additional Results

a) Models:

For MNIST, we use the standard LeNet5 implementation based on https://github.com/erykml/medium_articles. It has 61.7K parameters. We use the standard SGD with learning rate $= 1 \times 10^{-2}$ and a batch size of 100 to train the model for 20 epochs.

For CIFAR10, we use the VGG-mini and ResNet-mini implementations based on <https://github.com/nikhilbarhate99/Image-Classifiers>. VGG-mini has 5.75M parameters and ResNet-mini has 1.49M parameters. We first use the standard SGD with learning rate $= 1 \times 10^{-2}$ and a batch size of 100 to train the model for 20 epochs. We also use a modified SGD to train for 20 epochs, whose hyper-parameters are the same with additionally a weight decay of 5×10^{-4} , momentum of 0.9, and cosine learning rate scheduler based on https://pytorch.org/docs/stable/generated/torch.optim.lr_scheduler.CosineAnnealingLR.html.

b) MI Attacks:

We implement the LiRA attack based on https://github.com/tensorflow/privacy/tree/master/research/mi_lira_2021. For MNIST we train 16 `cnn32-3-max` shadow models with learning rate $= 0.001$ and a batch size of 64 for 20 epochs. For CIFAR10 we train 16 `wrn28-2` shadow models with learning rate $= 0.1$ and a batch size of 256 for 100 epochs. The MI score threshold is computed based on maximum accuracy.

We implement the EnhancedMIA attack based on https://github.com/privacytrustlab/ml_privacy_meter/blob/master/tutorials/population_metric.ipynb. The MI score threshold is computed to let the false positive rate $= 10\%$.

We implement the MEntr and Xent attacks based on <https://github.com/inspire-group/membership-inference-evaluation>. We implement the MIDA attack based on https://github.com/yigitcankaya/augmentation_mia. The label-specific MI score thresholds are computed based on maximum accuracy.

Algorithm 3 Generation of PoRs (Complete)

1: **Inputs:** $D = \{x_1, \dots, x_n\}$ - Training dataset; τ - Total number of iterations; $B_*^{(t)}$ - Training mini-batches for the t -th iteration where $t \in [\tau]$; $\text{Flip}(B_*^{(t)})$ - Binary flags indicating whether random horizontal flip augmentation has been applied to the samples in $B_*^{(t)}$; b - Size of each mini-batch, $|B_*^{(t)}|$; $\theta^{(0)}$ - Initialization parameters.

2: **Hyper-parameters:** $\text{step_size}^{(t)}$ - Learning rate at step t ; momentum - Momentum coefficient; weight_decay - Weight decay coefficient; κ - Number of splits; μ - Number of candidate mini-batches sampled every iteration for forging.

3: **for** $t = 1, \dots, \tau$ **do**

4: Compute gradients and update the original model:

5:

$$\text{grad}^{(t)} = \nabla_{\theta} \left(\frac{1}{b} \sum_{x \in \text{Aug}(\text{Flip}(B_*^{(t)}), B_*^{(t)})} \ell(x; \theta^{(t)}) + \text{weight_decay} \cdot \|\theta^{(t)}\|_2^2 \right),$$
$$\theta^{(t)} = \theta^{(t-1)} - \text{step_size}^{(t)} \cdot (\text{grad}^{(t)} + \text{momentum} \cdot \text{velocity}^{(t-1)}).$$

6: Randomly split $D = D_1^{(t)} \cup \dots \cup D_{\kappa}^{(t)}$ that satisfy Eqs. (5) and (6).

7: **for** $k = 1, \dots, \kappa$ **do**

8: Randomly select subset D_{sub} from $D \setminus D_k^{(t)}$.

9: Randomly select μ mini-batches with size b from D_{sub} : $B_1^{(k,t)}, \dots, B_{\mu}^{(k,t)}$.

10: **for** $m = 1, \dots, \mu$ **do**

11: Sample $\text{Flip}(B_m^{(k,t)}) \in \text{Uniform}(\{0, 1\}^b)$.

12: **end for**

13: Choose the best mini-batch and augmentation variables to approximate the gradient:

14:

$$m_*^{(k,t)} = \arg \min_{m \in [\mu]} \left\| \nabla_{\theta} \left(\frac{1}{b} \sum_{x \in \text{Aug}(\text{Flip}(B_m^{(k,t)}), B_m^{(k,t)})} \ell(x; \theta^{(t)}) + \text{weight_decay} \cdot \|\theta^{(t)}\|_2^2 \right) - \text{grad}^{(t)} \right\|_2^2.$$

15: **for** $x_i \in D_k^{(t)}$ **do**

16: **if** $x_i \in B_*^t$ **then**

17: $B_{\text{forge}}^{(t)}(x_i) = B_{m_*^{(k,t)}}^{(k,t)}$, $\text{Flip}(B_{\text{forge}}^{(t)}(x_i)) = \text{Flip}(B_{m_*^{(k,t)}}^{(k,t)})$;

18: **else**

19: $B_{\text{forge}}^t(x_i) = B_*^t$, $\text{Flip}(B_{\text{forge}}^t(x_i)) = \text{Flip}(B_*^t)$.

20: **end if**

21: **end for**

22: **end for**

23: **end for**

24: **Return:** original model $\theta_* = \theta^{(\tau)}$; all forged mini-batches $\{B_{\text{forge}}^{(t)}(x_i) : i \in [n], t \in [\tau]\}$; all augmentation variables $\{\text{Flip}(B_{\text{forge}}^{(t)}(x_i)) : i \in [n], t \in [\tau]\}$.

c) *Metrics:*

The MI prediction difference metric is measured in three settings: Diff, Common, and Validation. In the Common setting, as it is computationally expensive to look at all points in D_{-i} , we look at a random subset instead. The total number of MI predictions checked is $5n$. We do the similar in the Common setting.

The additional MI score difference metrics are shown in the box plots below. Outliers are not displayed in the box plots.

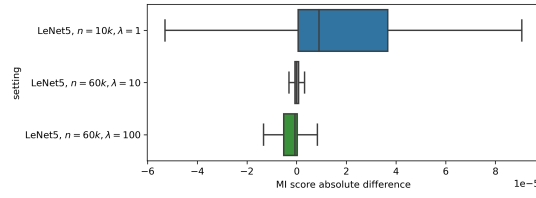


Fig. 7: Box plots of MEntr score differences ($s_{\mathcal{A}}$) on MNIST.

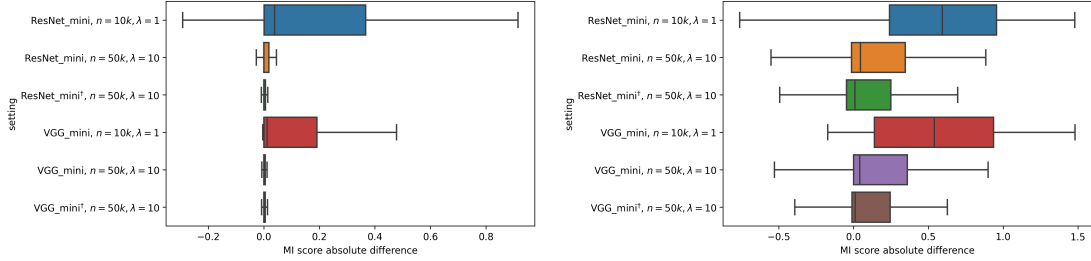


Fig. 8: Box plots of Mentr (left) and MIDA (right) score differences ($s_{\mathcal{A}}$) on CIFAR10 (\dagger means the modified SGD is used).

D. Indistinguishability of Mini-batches

Here, we describe why standard two-sample statistical tests, such as the Kolmogorov-Smirnov, test are not suitable for distinguishing between the forged mini-batches and the ones obtained from the original training (following standard SGD). The reason behind this is that mini-batches trained under standard SGD do not follow any fixed distribution and rather depends on the specificities of the exact practical implementation of SGD. For example, if we randomly sample mini-batches with no replacement (i.e. a mini-batch has to contain different samples), the frequency distribution is shown as the yellow curve in Fig. 9. On the other hand, if the SGD is implemented as a for loop of the dataloader in PyTorch, then the sample frequencies are uniform, as shown in the green curve in Fig. 9. Based on our empirical evaluation, the forged mini-batches have a frequency distribution (shown in the blue curve in Fig. 9 which lies in between the two aforementioned curves). Hence, running any two-sample test will almost certainly output a negative result (i.e., the two distributions are not the same). However, the forged mini-batches are very uniform and it is plausible that there exists a specific implementation of SGD – for example, a for loop implementation corresponding to a distributed training setting – that yields a similar distribution. Therefore, in this paper, we conjecture that one cannot disprove the validity of any distribution (i.e., the distribution corresponds to a valid SGD training) that lies between the green and yellow curves.

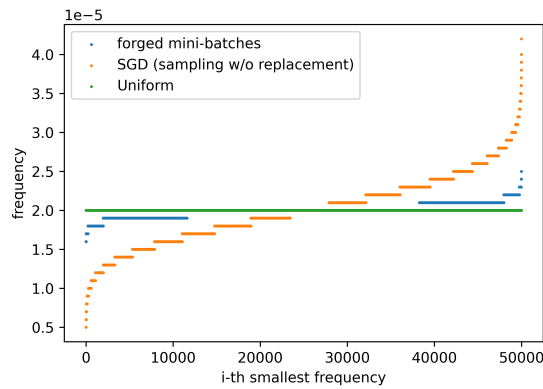


Fig. 9: Sorted sample frequencies of mini-batches from various processes.